Iterative calculations of dielectric eigenvalue spectra

Hugh F. Wilson,[1] Deyu Lu,[1] François Gygi,[2] and Giulia Galli[1]

[1]*Department of Chemistry, University of California–Davis, Davis, California 95616, USA*
[2]*Department of Applied Science, University of California–Davis, Davis, California 95616, USA*

The eigenvalues and eigenvectors of the dielectric matrix ϵ provide a compact representation of the screening properties of interacting electronic systems. We have previously shown that the dielectric eigenvalue spectrum may be efficiently computed by iterative linear-response calculations and that for nonmetallic systems ϵ may be obtained through an eigenvalue-eigenvector decomposition where only a small number of eigenvalues are included. Here we investigate the spectral properties of the dielectric matrices of a variety of systems (solids, nanostructures, and molecules) as well as the convergence properties of the eigenvalue decomposition of ϵ as a function of the number of eigenmodes. Our results provide guidance on how to perform practical calculations of dielectric matrices using iterative techniques.

I. INTRODUCTION

Within the linear-response theory, the dielectric matrix provides a complete representation of the electronic polarization and screening behavior of an interacting electronic system subject to external perturbations. Calculation of dielectric matrices is a key step in the determination of many properties of solids and nanostructures, e.g., excited-state and correlation properties. Particular applications of interest are, for example, the evaluation of quasiparticle energies in GW calculations[1] and of several other spectroscopic quantities[2] and the determination of screening properties in nanoscale electronic systems such as thin-film- or nanowire-based transistors and high-k dielectric layers.[3]

Most evaluations of static dielectric matrices $\epsilon(\mathbf{r},\mathbf{r}')$ of solids[4–7] have been performed using the approach pioneered by Adler[8] and Wiser[9] (AW) based on perturbation theory and the random-phase approximation (RPA). Using a plane-wave representation, the Fourier transform of the static RPA dielectric matrix of a nonmetallic system is given by[7]

$$\epsilon_{\mathbf{G},\mathbf{G}'}(\mathbf{q}) = \delta_{\mathbf{G},\mathbf{G}'} - \frac{4\pi e^2}{|\mathbf{q}+\mathbf{G}|^2}\frac{4}{N_k\Omega}\sum_{\mathbf{k},v,c} \frac{\langle v,\mathbf{k}|e^{-i(\mathbf{q}+\mathbf{G})\cdot\mathbf{r}}|c,\mathbf{k}+\mathbf{q}\rangle\langle c,\mathbf{k}+\mathbf{q}|e^{i(\mathbf{q}+\mathbf{G}')\cdot\mathbf{r}'}|v,\mathbf{k}\rangle}{E_{v,\mathbf{k}} - E_{c,\mathbf{k}+\mathbf{q}}}, \tag{1}$$

where Ω is the volume of the unit cell, $\mathbf{k}$ and $\mathbf{q}$ are wave vectors, and $\mathbf{G}(\mathbf{G}')$ denotes the reciprocal-lattice vectors. Each matrix element of $\epsilon(\mathbf{q})$ may be computed by performing the direct sum over single-particle conduction (c) and valence (v) bands with $E_{c,\mathbf{k}+\mathbf{q}}$ and $E_{v,\mathbf{k}}$ being the corresponding orbital energies, and we refer to this approach as the explicit summation approach (ESA). According to Eq. (1), the cost to compute each matrix element scales as $N_kN_cN_v$, where N_k is the number of k points used in the Brillouin-zone sampling and N_v (N_c) is the number of single-particle-occupied (empty) states. In principle, N_c included in the sum of Eq. (1) is infinite, however practical calculations of ϵ have been carried out by truncating the sum over the conduction bands at a finite number. Calculations of ϵ under the ESA have also been extended[7,10] beyond the RPA to include exchange-correlation effects in the response. In addition to the ESA so-called "direct" methods have been applied[11–13] to compute the dielectric response, where individual columns of $\epsilon(\mathbf{q})$ are obtained one at a time via the evaluation of the response to applied plane-wave potentials.

Despite the wide use of the ESA in recent years, there are technical issues that prevent its applicability to systems whose description requires a high-energy cutoff and/or large supercells. A major drawback of the ESA is that very large N_c is usually required to converge the summation in Eq. (1). For instance, even in the case of molecules with few atoms, in order to compute quasiparticle energies, typically about 1000 Kohn-Sham empty states are used to evaluate ϵ.[14,15] In addition, in many applications one needs to compute a functional form of ϵ instead of ϵ itself. For example, one wants to compute ϵ^{-1} in GW calculations and $\log(\epsilon)$ in RPA correlation-energy calculations[16] using the adiabatic connection fluctuation-dissipation theorem (ACFDT).[17,18] This involves expensive operations such as matrix inversion in the former case and full diagonalization in the latter case.[19]

In a recent work,[20] we have proposed a method for computing ϵ of a given system called the projective dielectric eigenpotential method (PDEP). In this approach, a finite number of eigenmodes of ϵ are obtained via an orthogonal iteration procedure implemented within density functional perturbation theory (DFPT).[21] For many classes of system,

the PDEP method is expected to be significantly more efficient than an ESA as long as a relatively small number of eigenvalues and eigenvectors are needed to reconstruct the full dielectric matrix with good accuracy. In this paper we address in detail the convergence properties of the PDEP method for several systems including bulk solids, nanostructures, and molecules. We also address efficiency issues of the PDEP and ESA and provide guidance in the selection of appropriate parameters for practical calculations.

The rest of the paper is organized as follows. In Sec. II we describe the theoretical background to the PDEP method and details of our current implementation. In Sec. III we present calculations of dielectric eigenvalue spectra of several bulk systems, nanostructures, and molecules. Sections IV and V contain a discussion of the convergence properties of the PDEP and ESA, respectively. Finally Sec. VI concludes our paper.

II. THEORETICAL BACKGROUND

Although PDEP can be applied to compute the eigenvalues and eigenvectors of a general dielectric matrix,[22] in the following we focus our discussion on the zero-frequency limit. The RPA dielectric matrix can be represented by an eigenvalue-eigenvector decomposition, and we call the set of eigenvalues the *dielectric eigenvalue spectrum*. While ϵ is not Hermitian, an Hermitian form (the so-called Hermitian dielectric matrix $\widetilde{\epsilon}$) can be obtained by a similarity transformation,

$$\widetilde{\epsilon}_{\mathbf{G},\mathbf{G}'}(\mathbf{q}) = \frac{|\mathbf{q}+\mathbf{G}|}{|\mathbf{q}+\mathbf{G}'|} \epsilon_{\mathbf{G},\mathbf{G}'}(\mathbf{q}), \tag{2}$$

and thus all eigenvalues of both $\widetilde{\epsilon}$ and ϵ are real. Furthermore, under RPA it can be shown[6] that the eigenvalues of ϵ are greater than or equal to 1. In prior works the dielectric eigenvalues of a number of systems, including bulk semiconductors and simple molecules, have been obtained[4–7,23] by diagonalizing $\widetilde{\epsilon}$.

The PDEP methodology instead uses an orthogonal iteration procedure to find the eigenvalues (λ_i) and eigenvectors ($\widetilde{\mathbf{v}}_i$) of $\widetilde{\epsilon}$ via repeated application of the $\widetilde{\epsilon}-I$ operator to a set of trial potentials, where I is the identity operator. If we label the dimension of $\widetilde{\epsilon}$ as N, we have

$$\widetilde{\epsilon} = \sum_{i=1}^{N} \widetilde{\mathbf{v}}_i \lambda_i \widetilde{\mathbf{v}}_i^H = \sum_{i=1}^{N} \widetilde{\mathbf{v}}_i (\lambda_i - 1) \widetilde{\mathbf{v}}_i^H + I. \tag{3}$$

In practice, the summation is truncated at $N_{\mathrm{eig}} \leq N$ and N_{eig} has to be chosen carefully to ensure the desired numerical accuracy.

The action of $\widetilde{\epsilon}$ on any arbitrary potential can be evaluated using DFPT. Within the linear-response regime $\epsilon = I - v_c \chi_0$, where v_c is the Coulomb kernel and χ_0 is the irreducible polarizability describing the response of the charge density $n(\mathbf{r})$ to the perturbation of the self-consistent field, i.e., $\Delta n = \chi_0 \Delta V_{\mathrm{SCF}}$. The response to the external field is given by $\Delta n = \chi \Delta V_{\mathrm{ext}}$, where the reducible polarizability χ satisfies Dyson's equation $\chi = \chi_0 + \chi_0(v_c + f_{\mathrm{xc}})\chi$. The exchange and correlation kernel f_{xc} is set at zero within the RPA, and one

has $\epsilon^{-1} = I + v_c \chi$. It is convenient to express Δn in terms of the variation in occupied Kohn-Sham orbitals $\Delta \psi_v(\mathbf{r})$. Keeping only terms linear in $\Delta \psi_v(\mathbf{r})$, we have

$$\Delta n(\mathbf{r}) = 4 \ \mathrm{Re} \sum_v \psi_v^*(\mathbf{r}) \Delta \psi_v(\mathbf{r}). \tag{4}$$

Finally $\Delta \psi_v(\mathbf{r})$ can be obtained by solving the linear system[21]

$$(H_{\mathrm{SCF}} + \alpha P_v - E_v)|\Delta \psi_v\rangle = -P_c \Delta V_{\mathrm{SCF}}|\psi_v\rangle, \tag{5}$$

where $H_{\mathrm{SCF}} = \frac{\mathbf{p}^2}{2m} + V_{\mathrm{SCF}}$ is the unperturbed Kohn-Sham Hamiltonian and P_v (P_c) is the projector onto the occupied (empty-)state manifold. The value of α is chosen such that the left-hand side of Eq. (5) is nonsingular. The application of Eqs. (4) and (5) to periodic systems is discussed in detail in Ref. 21.

As Eqs. (4) and (5) allow us to compute the charge-density response Δn from ΔV_{SCF}, the action of $\epsilon - I$ on any trial potentials can be obtained conveniently as $(\epsilon - I)\Delta V_{\mathrm{SCF}} = -v_c \chi_0 \Delta V_{\mathrm{SCF}} = -v_c \Delta n$. Finally, $(\widetilde{\epsilon} - I)\Delta V_{\mathrm{SCF}}$ is associated to $(\epsilon - I)\Delta V_{\mathrm{SCF}}$ through the connection in Eq. (2). Alternatively, one may consider to apply the DFPT on χ through $(\epsilon^{-1} - I)\Delta V_{\mathrm{ext}} = v_c \chi \Delta V_{\mathrm{ext}} = v_c \Delta n$, where ΔV_{ext} are treated as trial potentials. However, this route requires a self-consistent construction of ΔV_{SCF} in Eq. (5) which, from a computational standpoint, is more demanding than the previous procedure. For this reason, the dielectric eigenvalue spectra are computed from χ_0 instead of χ in the PDEP approach. Once the response $(\widetilde{\epsilon} - I)\Delta V_{\mathrm{SCF}}$ are solved, one may apply an orthogonal iteration procedure to obtain λ_i and $\widetilde{\mathbf{v}}_i$. It is important that such a procedure is applied to $\widetilde{\epsilon}$ and not to ϵ itself since ϵ is not Hermitian and therefore its eigenvectors are in general not orthogonal.

To compute the leading N_{eig} eigenmodes (with the highest N_{eig} eigenvalues) of $\widetilde{\epsilon}$, we begin with a set of initial trial potentials and iteratively apply the $\widetilde{\epsilon} - I$ operator. Ritz acceleration[24] is employed in the orthogonal iteration procedure, which provides faster convergence than the bare orthogonal iteration in situations where the density of eigenvalues becomes high in the region of interest. In principle the initial trial potentials may be any set of mutually orthogonal potentials provided that none is orthogonal to the subspace spanned by the first N_{eig} eigenpotentials. In practice we find that initial potentials composed of the product of plane waves and $n(\mathbf{r})$, plus a small amount of random noise, work efficiently.

It has been shown that[20] the computational effort for calculating $\widetilde{\epsilon}$ with N_{eig} eigenmodes scales as $N_{\mathrm{eig}} N_{pw} N_v^2$, where N_{pw} is the size of the wave-function basis set. This compares favorably with the scaling of $N_{pw}^2 N_v N_c$ in the ESA, particularly for systems requiring large basis sets and/or large unit cells. We note that the PDEP method can be parallelized very efficiently by carrying out the calculations of different eigenmodes on different processors.
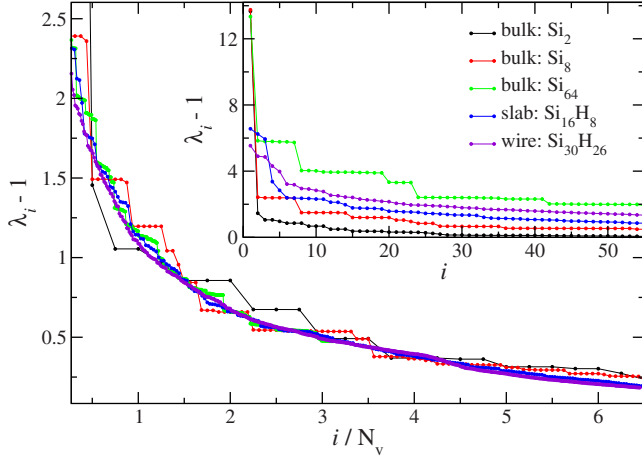
FIG. 1. (Color online) Dielectric eigenvalue spectra of bulk silicon and silicon nanostructures. λ_i denotes the eigenvalues of the dielectric matrix, and the eigenmode index i is scaled by N_v, the number of valence states. The unscaled curves are shown in the inset.
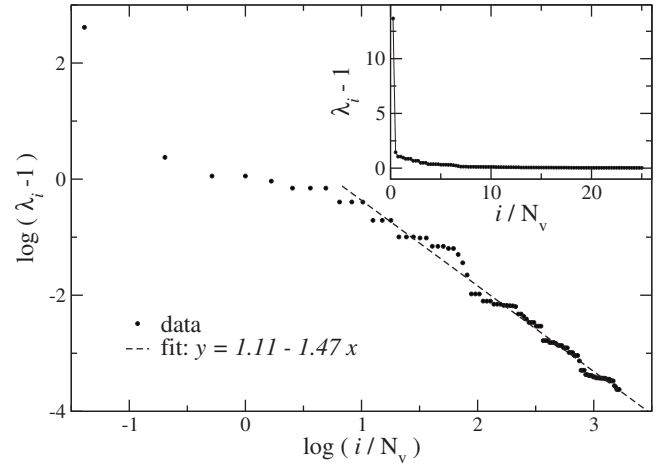

FIG. 2. Tail of the dielectric eigenvalue spectrum of bulk silicon (two-atom cell). The full spectrum is given in the inset. A fit to the data is provided, based on the Lindhard dielectric function (see text). Labels i, λ_i, and N_v have the same meaning as in Fig. 1.

III. DIELECTRIC EIGENVALUE SPECTRA OF SOLIDS, MOLECULES, AND NANOSTRUCTURES

In the following we analyze the dielectric eigenvalue spectra and convergence properties of several systems, as obtained with the PDEP technique. In particular, we study three bulk solids: silicon (two-atom, eight-atom and 64-atom unit cells), diamond carbon (eight-atom unit cell), and NaCl (eight-atom unit cell); three isolated molecules: H_2O, benzene, and Si_5H_{12}; and two nanostructured materials, a 1.1 nm hydrogen-terminated silicon slab ($Si_{16}H_8$) and a 1.2 nm hydrogen-terminated silicon nanowire ($Si_{30}H_{26}$).

The ground-state properties were obtained using the program PWSCF in the QUANTUM-ESPRESSO package[25] and the PDEP calculations were performed based on a modified version of the "PHONON" code in the same package. Plane-wave basis sets were used throughout with cutoffs of 12 Ry for the silicon/hydrogen systems, 50 Ry for the carbon systems, 60 Ry for the systems containing oxygen, and 40 Ry for the NaCl system. The Brillouin-zone sampling was done as follows: we used 64 k points in the full Brillouin zone for each of the eight-atom Si, C, and NaCl unit cells and kept the same effective density of k points for each of the other periodic or semiperiodic structures considered in this work. This amounts to using 256 k points for the two-atom bulk Si cell, 4 k points for the 64-atom Si cell, and 4 and 16 k points respectively for the nanowire and nanoslab geometries.[26]

Although the PDEP method can be applied to $\tilde{\epsilon}(\mathbf{q})$ at arbitrary $\mathbf{q}$, in this paper we focus on cases where $\mathbf{q} \rightarrow 0$. We chose $\mathbf{q}$ in the plane in the nanoslab calculation and along the growth direction in the nanowire calculation. Except when noted otherwise, we consider the iterative procedure converged when the relative error in eigenvalues $|\delta\lambda_i/\lambda_i|$ in two successive PDEP iterations is less than 10^{-6}.

A major advantage of PDEP in computing the full $\tilde{\epsilon}$ matrix is based on the assumption that $N_{eig} \ll N_{pw}$. In order to achieve a high accuracy, this requires that the quantity ($\lambda_i -1$) decays very rapidly to zero as i increases. In this section, we investigate the dielectric eigenvalue spectra of a wide variety of systems and show that indeed this assumption is well justified.

The dielectric eigenvalue spectra of silicon-based materials (bulk silicon, a slab, and a nanowire) are shown in the inset of Fig. 1. The PDEP results for bulk silicon are in very good agreement with previous ESA calculations.[6,7,20] We first consider the bulk spectra obtained from different unit cells. For each system, the total number of dielectric eigenmodes is N_{pw}. At a given kinetic-energy cutoff $N_{pw} \propto \Omega$, where Ω is the volume of the unit cell. The inset of Fig. 1 clearly shows that the larger the Ω, the slower the decay rate. For the purpose of comparison, it is therefore more convenient to rescale the eigenmode index so that it becomes Ω independent. As $\Omega = \frac{4}{3}\pi r_s^3 \times (2N_v)$, where r_s is the Wigner-Seitz radius, a natural choice is to use a running index i/N_v. As we can see in Fig. 1 the dielectric spectra of Si-based systems fall approximately on the same curve after the rescaling of the eigenmode index.

The use of the rescaling adopted for bulk systems in the case of nanostructures is not straightforward since the supercell contains an arbitrary amount of empty space, and consequently Ω is not well defined. However one may introduce an effective unit-cell volume assuming an average r_s to be the same as in bulk Si, i.e., $\Omega_{eff} = \frac{4}{3}\pi r_s^3 \times (2N_v)$. When the index for nanostructures is scaled in the same way as in the bulk, all the dielectric spectra of Si-based systems show the same decaying behavior, as demonstrated in Fig. 1.

The convergence properties of PDEP regarding N_{eig} is related to the decay behavior of the dielectric eigenvalue spectra at large i. In order to approximately characterize the tail of spectra for solids, we consider the Lindhard dielectric function[27] of the homogeneous electron gas. Thus one has $\epsilon(\mathbf{q}) - 1 \propto 1/q^2$ in the long-wavelength limit and $\epsilon(\mathbf{q}) - 1 \propto 1/q^4$ for $q \gg k_F$, where k_F is the Fermi wave vector. Unlike the response function of the homogeneous electron gas, which is diagonal in reciprocal space, $\tilde{\epsilon}$ of real solids has off-diagonal matrix elements due to so-called "local-field ef-
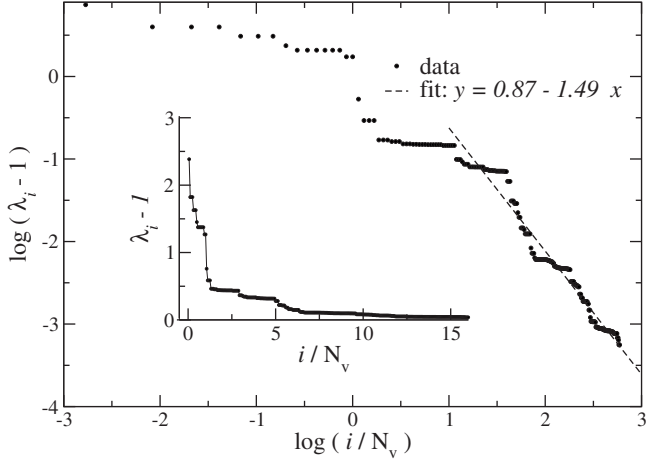
FIG. 3. Tail of the dielectric eigenvalue spectrum of bulk NaCl. The full spectrum is given in the inset. A fit to the data is provided based on the Lindhard dielectric function (see text). Labels i, λ_i, and N_v have the same meaning as in Fig. 1.

FIG. 5. (Color online) Dielectric eigenvalue spectra for H_2O, benzene, and Si_5H_{12}. Labels i, λ_i, and N_v have the same meaning as in Fig. 1.

fects." As a consequence the dielectric eigenvalues are in general different from the diagonal-matrix elements of ϵ. However, for perturbations with very large Fourier components, local-field effects usually become less relevant. Therefore we approximate the tail of the spectra by a Lindhard function to obtain $(\lambda_i - 1) \propto i^{-4/3}$, where $i \propto G^3$ for sufficiently large i. Figures 2–4 show the tail of the eigenvalue spectra for three different solids: silicon, NaCl, and diamond. These systems are chosen as representative semiconducting and insulating systems, with different types of bonding (covalent and ionic). Since we have shown that all the silicon spectra studied here have very similar decay behavior with proper scaling (see Fig. 1), here we only show the results of the two-atom Si cell. A common feature in Figs. 2–4 is that the spectra (inset) initially decay very rapidly and then flatten out as i increases. From fitting the tail of the dielectric eigenvalue spectra, we found that the $i^{-4/3}$ decay law is roughly

obeyed in all the three systems [with powers of 1.47, 1.49, and 1.36 for Si ($r_s = 3.16$), NaCl ($r_s = 3.31$), and C ($r_s = 2.07$), respectively].

The dielectric eigenvalue spectra of three molecular systems, H_2O, benzene, and Si_5H_{12}, are shown in Fig. 5. Similar to the nanostructures discussed above, the indices are scaled by N_v. We find the overall decay behavior is similar to that of solids and nanostructures, namely, a very rapid decay followed by a slow decline, although the decay behavior shows more significant diversity. It suggests that the eigenvalue-eigenvector decomposition method may be advantageous also in the case of molecular systems.

In this section we have demonstrated the existence of similar decay behavior in the dielectric eigenvalue spectra of several systems regardless of composition, size of band gap, or periodicity. The dielectric eigenvalue spectrum is largely dependent on the size and average electronic density of the system. This is a very important prerequisite for the applicability of the PDEP technique. However, in order to understand the utility and efficiency of the approach, one needs to know in practice how many eigenmodes are needed to compute properties of interest. Although it is not our goal to provide an exhaustive answer to this question, we provide several examples showing that rapid convergence of some excited-state and correlation-energy properties can be achieved by using a rather small number of eigenvectors and eigenvalues in Eq. (3). This is the subject of Sec. IV.

IV. CONVERGENCE PROPERTIES OF THE PDEP METHOD

In this section, we use the quasiparticle band gap and the RPA correlation energy of bulk silicon as examples to investigate the convergence of the eigenvalue-eigenvector decomposition of the dielectric matrix with respect to N_{eig}. In the first case, the quasiparticle direct gap of silicon was computed at the Γ point using the GW approximation[1] and the von der Linden and Horsch plasmon-pole model.[28] The dependence of the gap on N_{eig} is shown in Fig. 6(a), where it is
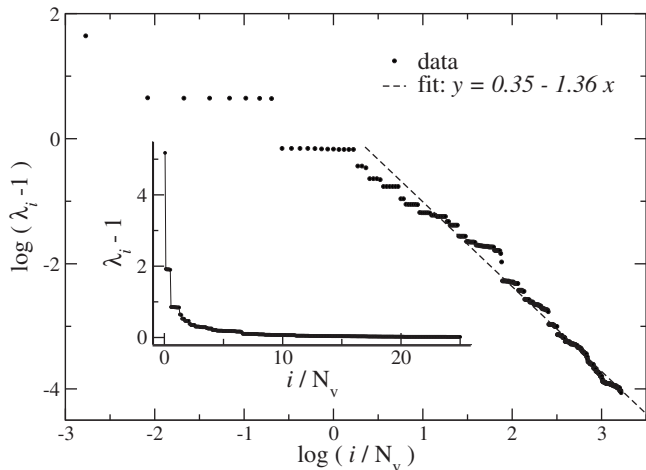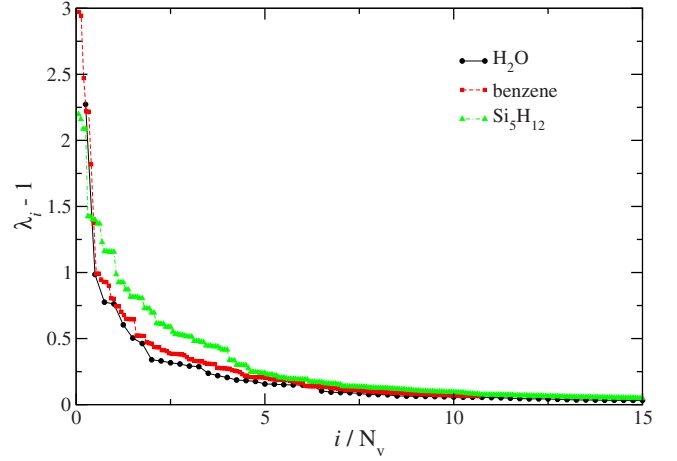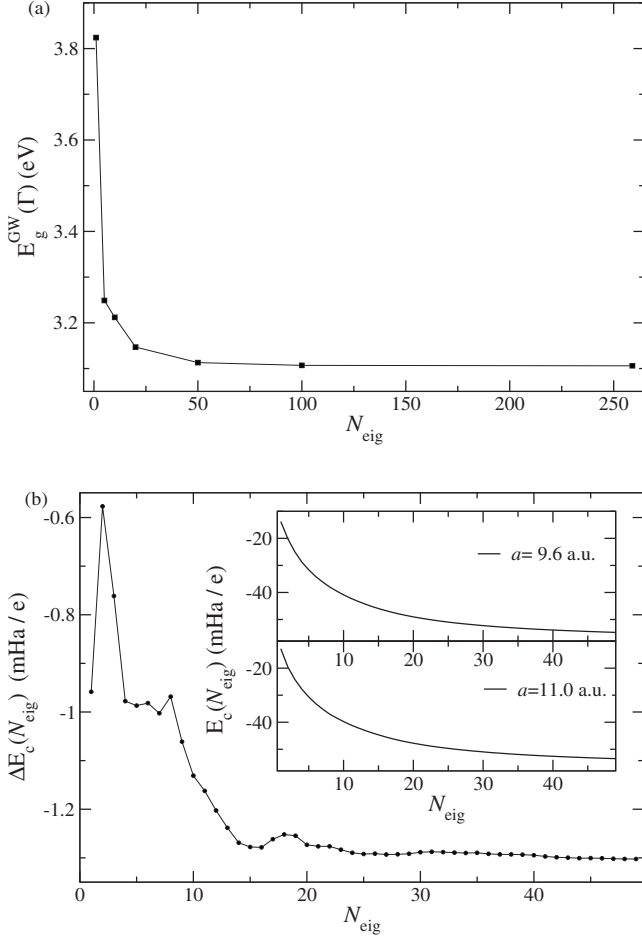

FIG. 4. Tail of the dielectric eigenvalue spectrum of bulk C in the diamond phase. The full spectrum is given in the inset. A fit to the data is provided based on the Lindhard dielectric function (see text). Labels i, λ_i, and N_v have the same meaning as in Fig. 1.

FIG. 6. (a) Quasiparticle gap (E_g^{GW}) of bulk silicon at the Γ point as a function of the number of eigenmodes N_{eig} included in Eq. (3). (b) Convergence of the relative and absolute (inset) RPA correlation energy of silicon with respect to N_{eig}. The correlation energy is computed from $E_c^{RPA} = \frac{1}{2\pi N_q} \int_0^\infty d\omega \Sigma_q \Sigma_j \{\log[\lambda_j(\mathbf{q}, i\omega)] - \lambda_j(\mathbf{q}, i\omega) + 1\}$ (Ref. 22), where λ_i denote eigenvalues of the dielectric matrix.

seen that only a small number of eigenmodes are needed (about 25) to reach an accuracy of 0.1 eV. A similar trend has also been found in quasiparticle calculations of liquid water and ice I*h*.[23] As a second example, we have computed the RPA correlation energy of bulk silicon at different lattice constants (a=9.6 and 11.0 a.u.) using the ACFDT. This requires generalizing the linear-response equation to imaginary frequencies and using more sophisticated iterative procedures to obtain the eigenvalues of the dielectric matrix than at ω=0. Details of these generalizations will be given elsewhere. Absolute energies, shown in the insets of Fig. 6(b), decay rather quickly and flatten out around $N_{eig} \approx 50$, while the energy difference shows an even weaker dependence on N_{eig} and appears to be converged for $N_{eig} \gtrsim 25$.

To assess the numerical error of the eigenvalue-eigenvector decomposition of $\tilde{\epsilon}$ as a function of N_{eig}, we define $\Delta\tilde{\epsilon}$ as the difference between the exact dielectric matrix and the approximate one constructed from N_{eig} eigenmodes and introduce two formal measures of the error on unconverged results: (1) the two norm of $\Delta\tilde{\epsilon}$, i.e., $\|\Delta\tilde{\epsilon}\|_2$
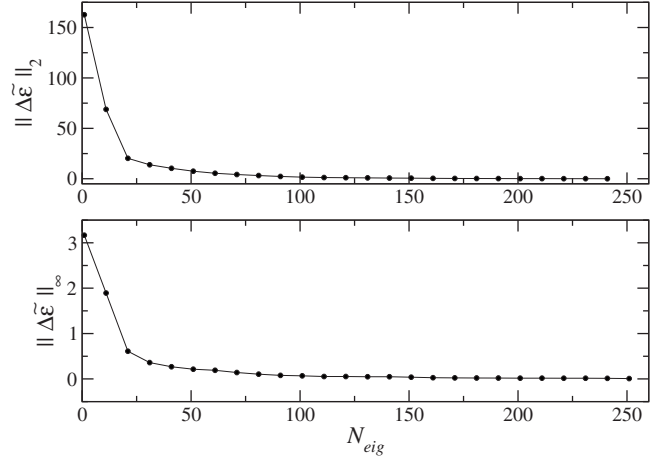

FIG. 7. Two norm and infinity norm of $\Delta\tilde{\epsilon}$ for the eight-atom cell bulk silicon. Here $\Delta\tilde{\epsilon}$ is the difference between the exact dielectric matrix and the approximate matrix constructed from N_{eig} eigenmodes.

$= (\Sigma_{ij} \Delta\tilde{\epsilon}_{i,j}^2)^{1/2}$; (2) the infinity norm of $\Delta\tilde{\epsilon}$ defined as the largest element of $|\Delta\tilde{\epsilon}_{i,j}|$.

In Fig. 7, we plot the two norm and infinity norm of $\Delta\tilde{\epsilon}$ of bulk silicon (the eight-atom cell) as a function of N_{eig}. To obtain the exact dielectric matrix, one needs about 750 eigenmodes. Since $\lambda_i - 1$ drops quickly toward zero as a function of i, we instead use 256 eigenmodes ($\lambda_{256} - 1$ =0.05 as compared to $\lambda_1 - 1$=13.75) to approximate the exact dielectric matrix. The magnitude of both norms decreases steadily as i increases and the onset of convergence around N_{eig}=50 is consistent with the results reported in Fig. 6 although the GW gap and the correlation-energy differences computed here appeared to be well converged even for N_{eig} less than 50.

V. CONVERGENCE PROPERTIES OF THE ESA

When $\tilde{\epsilon}$ is obtained from ESA, one needs to check convergence of the results with respect to N_c included in the
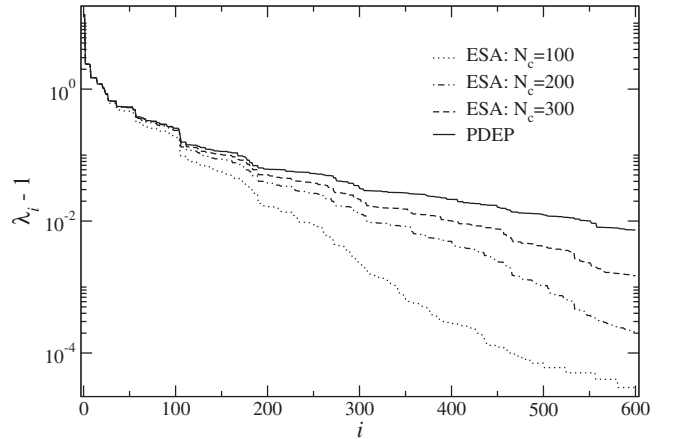

FIG. 8. Dielectric eigenvalue spectra for the eight-atom unit-cell bulk silicon computed by PDEP and by ESA [see Eq. (1)] using three different values for the number of conduction bands N_c. Labels i, λ_i, and N_v have the same meaning as in Fig. 1.
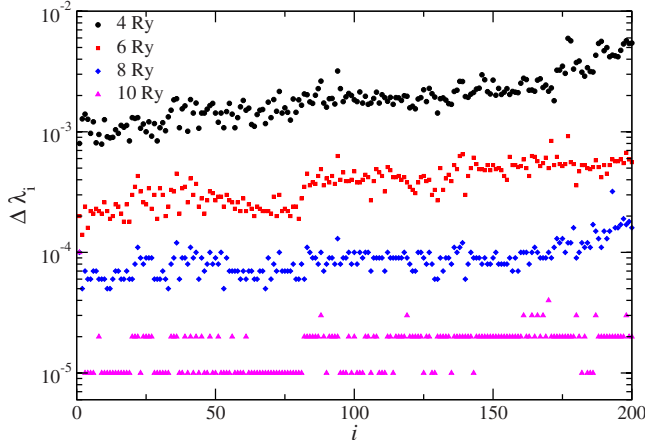
FIG. 9. (Color online) Difference between the dielectric eigenvalues ($\Delta \lambda_i$) using a 12 Ry cutoff and those obtained using basis sets of 4, 6, 8, and 10 Ry.

summation of Eq. (1) and the energy cutoff used to represent the matrix. In many calculations in the literature, $\widetilde{\epsilon}$ is represented by using a smaller basis set than that employed for the representation of the Kohn-Sham wave functions. This is often necessary due to memory requirements and prohibitive CPU requirements in inverting dielectric matrices with dimension larger than approximately 10 000.

We first check the convergence with respect to N_c by comparing the dielectric eigenvalue spectra computed using Eq. (1) to those obtained by the PDEP method for the eight-atom bulk silicon system. The same Kohn-Sham ground state was used in both calculations. The results in Fig. 8 are plotted on a logarithmic scale in order to emphasize the differences. As one can see the ESA results gradually converge to the PDEP ones as N_c is increased, and the rate of convergence is in general faster for highest-lying eigenvalues.

As mentioned above, in ESA $\widetilde{\epsilon}$ is often computed from a basis set smaller than that of the single-particle wave functions. In the following we investigate the effect of truncating the size of the $\widetilde{\epsilon}$ matrix in **G** space. We consider once again the eight-atom Si cell; since this system is sufficiently small, we can easily calculate the full $\widetilde{\epsilon}$ matrix with the 12 Ry cutoff used for the wave functions. In Fig. 9 we plot the difference between the eigenvalues generated in the ESA with a 12 Ry cutoff and those generated with 4, 6, 8, and 10 Ry. Except for the smallest cutoff (4 Ry) $\Delta \lambda_i$ are almost constant as a function of i, and for $E_{cut} \geq 8$ Ry the absolute

value of these differences appear to be rather small. These results may provide a justification, *a posteriori*, of the relatively small cutoff used in the literature to evaluate dielectric matrices in those systems.

VI. CONCLUSIONS

In this paper we have discussed a technique to compute iteratively the dielectric eigenvalue spectra of interacting electronic systems and thus to provide an eigenvalue-eigenvector representation of dielectric matrices. This technique, which we referred to as PDEP, is based on the solution of the linear-response equation within density-functional perturbation theory and does not require lengthy calculations of single-particle empty states nor the inversion of dielectric matrices. The efficiency of the PDEP approach compared, e.g., to explicit summation approaches, relies on the assumption that only a relatively small number of eigenvectors and eigenvalues are needed to provide an accurate representation of the dielectric matrix. We have presented calculations of dielectric spectra for representative solid, nanostructured, and molecular systems and we have shown that they all exhibit fast decays of the eigenvalues toward unity, thus providing a justification for the use of the PDEP approach at least for the classes of systems studied here. In addition, we have presented representative GW and correlation energy calculations for Si showing that for practical purposes the convergence of PDEP as a function of the number of eigenmodes is even faster than that predicted by the decay of dielectric spectra, and that very accurate results may be obtained just by reconstructing the dielectric matrix using as few as 30–50 eigenpotentials. These results are consistent with those obtained by detailed analysis of two-norm and infinity-norm convergence tests conducted on representative dielectric matrices. Our findings show that PDEP is a promising technique to compute dielectric-matrix spectra for systems requiring large basis sets and/or large supercells and that can be efficiently employed in, e.g., excited-state and correlation-energy calculations.

[1] L. Hedin, Phys. Rev. **139**, A796 (1965).

[2] A. Diebold, *Handbook of Silicon Semiconductor Metrology* (CRC, New York, 2001).

[3] F. Giustino and A. Pasquarello, Phys. Rev. B **71**, 144104 (2005).

[4] A. Baldereschi and E. Tosatti, Phys. Rev. B **17**, 4710 (1978).

[5] A. Baldereschi and E. Tosatti, Solid State Commun. **29**, 131 (1979).

[6] R. Car, E. Tosatti, S. Baroni, and S. Leelaprute, Phys. Rev. B **24**,

985 (1981).

[7] M. S. Hybertsen and S. G. Louie, Phys. Rev. B **35**, 5585 (1987).

[8] S. L. Adler, Phys. Rev. **126**, 413 (1962).

[9] N. Wiser, Phys. Rev. **129**, 62 (1963).

[10] S. Baroni and R. Resta, Phys. Rev. B **33**, 7017 (1986).

[11] K. Kunc and E. Tosatti, Phys. Rev. B **29**, 7045 (1984).

[12] A. Fleszar and R. Resta, Phys. Rev. B **31**, 5305 (1985).

[13] L. Reining, G. Onida, and R. W. Godby, Phys. Rev. B **56**, R4301

(1997).

[14] M. L. Tiago and J. R. Chelikowsky, Phys. Rev. B **73**, 205334 (2006).

[15] Y. Li, D. Lu, and G. Galli, J. Chem. Theory Comput. **5**, 881 (2009).

[16] Y. M. Niquet, M. Fuchs, and X. Gonze, Phys. Rev. A **68**, 032507 (2003).

[17] D. C. Langreth and J. P. Perdew, Solid State Commun. **17**, 1425 (1975).

[18] D. C. Langreth and J. P. Perdew, Phys. Rev. B **15**, 2884 (1977).

[19] J. Harl and G. Kresse, Phys. Rev. B **77**, 045136 (2008).

[20] H. F. Wilson, F. Gygi, and G. Galli, Phys. Rev. B **78**, 113303 (2008).

[21] S. Baroni, S. de Gironcoli, A. Dal Corso, and P. Giannozzi, Rev. Mod. Phys. **73**, 515 (2001).

[22] D. Lu, Y. Li, D. Rocca, and G. Galli, Phys. Rev. Lett. **102**, 206411 (2009).

[23] D. Lu, F. Gygi, and G. Galli, Phys. Rev. Lett. **100**, 147601 (2008).

[24] G. H. Golub and C. F. Van Loan, *Matrix Computations* (Johns Hopkins University Press, Baltimore, MD, 1983).

[25] P. Giannozzi *et al.*, http://www.quantum-espresso.org

[26] The dielectric matrix is known to be quite sensitive to k-point sampling (Ref. 5) and it should be noted that the k-point sampling given here results in an accuracy not better than a few percent, however we believe this is sufficient for illustrative purposes.

[27] J. Lindhard, K. Dan. Vidensk. Selsk. Mat. Fys. Medd. **28**, 8 (1954).

[28] W. von der Linden and P. Horsch, Phys. Rev. B **37**, 8351 (1988).